

Intracortical Origin of Visual Maps

U.A. Ernst¹, K.R. Pawelzik¹, C. Sahar-Pikielny^{2,3} and M.V. Tsodyks³

December 18, 2001

¹Institute for Theoretical Physics, University of Bremen, Kufsteiner Str., D-28334 Bremen, Germany

²School of Physics and Astronomy, Tel-Aviv University, Tel-Aviv 69978, Israel

³Department of Neurobiology, Weizmann Institute of Science, Rehovot 76100, Israel.

Address for correspondence:

M. Tsodyks

Department of Neurobiology

Weizmann Institute of Science

Rehovot 76100, Israel

Email misha@weizmann.ac.il

Tel +972-8-9342157

Fax +972-8-9344131

Abbreviations: PO, Preferred orientation; PD, Preferred direction; VF, Visual field.

Abstract

Recent experiments indicate that the shape of maps of preferred orientation in the primary visual cortex does not depend on visual experience. We propose a network model which demonstrates that the orientation and direction selectivity of individual units and the structure of the corresponding angle maps could emerge from local recurrent connections. Our model reproduces the structure of the maps of preferred orientation and preferred direction and explains the origin of their interrelation. The model also provides a novel explanation for the correlation between position shifts of receptive fields and changes of preferred orientations of single neurons across the surface of the cortex.

Neurons in primary visual cortex respond preferentially to elongated stimuli (1). The spike rate of a given cell depends on various features of the stimulus, such as position in visual space, its orientation and direction of motion. The response properties of neurons do not change significantly in a direction perpendicular to the surface of the cortex, such that one can think of these neurons as units forming a functionally uniform cortical "column". Across the surface, however, these response properties change smoothly, leading to the corresponding cortical maps (2,3). These maps appear early during development and exhibit characteristic patterns of mutual interrelations. According to the traditional theoretical thinking, the cortical maps result from an experience-dependent development of afferent and/or lateral connections (4-8). However, recent experiments failed to detect any significant effects of visual experience on the shape of orientation preference maps in kittens (9-11). In particular, the maps appear to be stable from the very first day they can be detected (9). In the experiments of (10), the orientation maps developed subsequently for the two eyes. The

resulting shape of the maps was identical, despite of the fact that the eyes were never opened simultaneously and therefore were not subjected to the same visual input. Finally, the orientation maps in binocularly deprived kittens had an overall appearance similar to normal maps (11). Taken together, these results strongly indicate the existence of some yet unknown factor which determines the ultimate shape of visual cortical maps before visual experience. A closely related issue is the mechanism of orientation and direction selectivity of individual neurons. While the original model of Hubel and Wiesel (1) proposed that a purely feed-forward arrangement of inputs is responsible for generating orientation selectivity, subsequent experimental and theoretical work indicated an important role for intracortical connections (see (12) for a recent review). No generally accepted neural model for directional selectivity of cortical neurons exists so far. The relative contribution of feed-forward and lateral processing to the orientation and direction selectivity of single cortical neurons remains a controversial topic.

In this contribution, we explore the idea that both orientation and direction selectivity of single neurons, as well as the shape of the corresponding maps, emerge from a stereotyped pattern of intra-cortical connections and are therefore independent from visual experience. To demonstrate that this is possible, we simulated a two-dimensional network of interconnected units (columns), which is supposed to mimic the primary visual cortex at the very first stages of development. Accordingly, the units in the network received inputs from rotationally symmetric input fields. In other words, in the absence of lateral connections within the network, the units do not exhibit any orientation or direction selectivity. Following (13,14), we assumed that intra-cortical connections induce lateral interactions having a mexican-hat

shape, i.e. excitation dominating on short distances followed by inhibition on longer ranges (Methods; see Fig. 2(a)). This arrangement was complemented with a random jitter in the connection strengths, resulting in random inhomogeneities in the lateral feedback. We then simulated the dynamics of activities in the network in response to oriented gratings moving in different directions. As we demonstrate in the next section, the response of single units acquired orientation and direction selectivity exclusively due to the lateral interactions. Moreover, the distribution of these selectivities across the network resulted in corresponding feature maps that shared the main properties of experimentally observed maps.

RESULTS

Network population states

As indicated by anatomical studies, geniculate afferents to a typical cortical cell are by far outnumbered by intracortical synapses (15). Correspondingly, we scaled the strength of interactions such that the dynamics of the activities depended more strongly on the intra-cortical interactions than on the afferent inputs. Under these conditions, any spatially extended stimulus evokes localized patches of increased activity separated by regions whose activity is inhibited (16).

Mathematically, this state of network activity arises when the interactions are strong enough such that the uniform state becomes unstable (13). Without inhomogeneities, the system is rotationally invariant, and therefore there is an infinite degeneracy of the steady activity states regarding arbitrary spatial shifts, i.e. every state is only marginally stable (13;

for simplicity, we exclude the role of the boundaries by applying periodic boundary conditions - see Methods). The presence of local inhomogeneities in the inter-unit connections breaks the symmetry and greatly reduces the set of possible states (17). The remaining states are the ones which maximize the amount of local excitatory feedback, subject to a global constraint on the average distance between the patches which is determined by the profile of interactions. The reduction in the set of states makes the network dynamics stable against random fluctuations. In particular, repeating the simulation with the same input but starting from random initial activations of units consistently led to the same pattern of patches, provided the amplitude of initial activations was not too big (not shown).

Orientation selectivity

We were particularly interested in the response of the network to moving full-field gratings. For every spatial configuration of the grating, different subsets of neurons receive different levels of afferent excitation. The configuration of the activity patches will then be selected by the combination of afferent and recurrent excitation, again with the global constraint on the minimal distance between patches. Hence for each orientation of the grating, the afferent inputs effectively select a particular pattern of activity patches (Fig. 2(b)).

Importantly, the positions of active patches are robust against different random initial conditions due to the stabilizing effect of the inhomogeneities in the lateral connections (17). Since the stable positions of the patches are different for different orientations of the grating, individual units in the network acquire orientation selectivity, i.e. the activity of each unit depends on the orientation of the stimulus (Fig. 2(c)). Moreover, nearby units tend to prefer similar orientations due to the spatial compactness of the activity patches.

We summarized these results by computing the *preferred orientation* (PO) of each unit as the orientation causing its maximal activation (see Methods), to obtain a PO angle map (Fig. 2(c)). One can clearly see regions where PO varies continuously across the network. Furthermore, there are points and lines where the PO changes abruptly which are called pinwheels and fractures, respectively. These singularities appear near places where patches of activity corresponding to different orientations come close to each other. The overall layout of the resulting maps is similar to that of experimentally obtained PO maps (18,19).

Direction selectivity

To study the direction selectivity, we considered the difference in the response of the network to two opposite directions of movement of an equally oriented grating. Here again, the local inhomogeneities in the connections play a crucial role in determining the nature of the response. Without them, the activity patches move across the network along with the stimulus. As explained above, inhomogeneities act to pin down the patches to particular positions determined by the strength of the local excitatory feedback. If the inhomogeneities are big enough, they act as barriers between neighboring configurations of the patches and the moving stimulus is then not able to shift the patches far from their most stable positions. Instead, one observes a pendulum-like oscillatory movement of the patches near their stable positions. The precise trajectory of a patch depends on both, the direction of the grating movement, and the direction in which, by means of the random inhomogeneities, lateral excitatory feedback is stronger. Thus, the average positions of each activity patch for two opposite directions of the stimulus movement are shifted relative to each other. Due to this effect, the set of units tuned to a particular orientation is divided into two subgroups, each

preferring opposite directions of stimulus movement (Fig. 3(a)). Necessarily, the deformation being roughly symmetrical, there has to be a narrow region within the activated area where the activities for stimuli moving in either of the two directions are the same (21). A similar relation between PO and PD cortical maps was recently observed in an experimental study (22).

The overall layout of directional preferences across the network is summarized in the *preferred directions* (PD) angle map (Fig. 3(b); see Methods). By subtracting the two activity patterns for opposite directions one obtains the differential map (Fig. 3(a), length of arrows). Comparing the average amplitude of this map with the corresponding differential map for two orthogonal orientations (not shown), we found that the orientation map was about twice as strong as the direction map, in agreement with the experimental results obtained for kittens (22). The relative weakness of the PD map in the network is a consequence of the strong pinning of the activity patches at the particular locations for a given orientation. As a result, the amplitude of the oscillatory movement of patches, and thus the amplitude of the corresponding differential map, is small.

Retinotopic organization and orientation map

We then tested the network response to spatially localized inputs (see Methods). We were interested in the relation between the arrangement of the receptive fields of individual units and the spatial scale of the orientation map. This issue was recently addressed experimentally in (23). The orientation map can be characterized by the typical size of a region which represents all orientations (hypercolumn). It is clear that the size of a hypercolumn equals the mean distance between columns having the same preferred orientation.

Two regions with the same preferred orientation in neighboring hypercolumns correspond to two adjacent activity patches for this orientation. We therefore conclude that the size of the hypercolumn is determined by the average distance between the patches. On the other hand, for a localized input which evokes just one activity patch, the units which are located at the opposite sides of the patch will be the closest units having non-overlapping receptive fields. This is because, by definition, the units which belong to the same patch are activated by the same location of the localized stimulus, i.e. their receptive fields have a certain degree of overlap, as opposed to the units on the opposite sides of the patch which are never activated by the single stimulus and therefore have non-overlapping receptive fields.

This reasoning indicates that the relation between the sizes of receptive fields and the orientation hypercolumns depends on the ratio between the size of the activity patches and the distance between them. In our simulations, the distance between the activity patches was about twice as large as the diameter of each patch (Fig. 1). Correspondingly, the smallest distance between two units with non-overlapping receptive fields should be about one half of the size of the hypercolumn. This relation was indeed observed in our simulations. In Fig. 4 we plot the distance between the receptive field centers, normalized by their size, for each pair of units in the network vs. the angle between their preferred orientations. One can see that the normalized distance of 1 (no overlap) corresponds to the angle of about 90 degrees between the preferred orientations. A similar dependency was reported in an experimental study (23). We emphasize that this dependency arises naturally from the fact that the response of the network to both spatially localized and extended stimuli is mainly determined by the population states of network activity and not by feedforward

connections (see also (24)). If the latter was the case, it is not clear how this particular relationship between the receptive fields of single units and the spatial scale of OP maps would be established.

Parameters and robustness of the model

Here we briefly discuss the meaning of the major parameters and their influence on the overall behavior of the model.

The main factors which determine the activity states of the network and spatial dimensions of the maps are the strength and profile of inter-unit interactions. Fig. 5 illustrates three different modes of network activity, for varying strengths of interactions. Orientation maps are observed in the marginal state, in which stereotyped activity patches emerge for any spatially extended stimuli. The region occupied by this state on the phase diagram expands when the ratio between the spatial scales of inhibition and excitation increases above one. We found numerically that in networks of our size, the robust maps were observed when the ratio was above 1.5. The average distance between the patches (i.e. the size of a hypercolumn) is mainly determined by the spatial scales of the excitatory and inhibitory flanks (Fig. 5, legend).

As described above, inhomogeneities play an important role in emergence of stable maps in the network. There are many ways inhomogeneities can be introduced in the model, and we tried different realizations leading to qualitatively identical results. In the simulations presented, the strength of connections had a mexican hat shape, perturbed by multiplicative random factors of variable amplitude (Methods). To study how general our results are, we did a series of control simulations varying the amplitude of the noise η (data not shown).

We found a whole interval of amplitudes leading to stable maps (with all other parameters as in Methods, the range was 12 % to 36 %). Intuitively, the inhomogeneities should be strong enough to stabilize the spatial locations of patches for a stimulus with a particular orientation, but still allow stimuli with different orientations to evoke different configurations of patches. The main result of the control simulations is, that for every noise amplitude in the allowed region, the overall appearance of the orientation and direction maps is very similar. This proves that it is the average profile of inter-unit interactions that determines the qualitative properties of the maps, and not the particular realization of the noise.

DISCUSSION

Our simulations demonstrate that local intra-cortical connections could be responsible for the orientation and direction selectivity of single cortical neurons, as well as for the geometrical shape of the corresponding maps at the very early stages of cortical development. This hypothesis is reinforced by the result that the overall appearance of the simulated maps, and the interrelation between them was the same as in experimentally observed maps. Since no activity-specific development of neither afferent nor lateral interactions was involved, the shape of the maps in our model is strictly a function of the pattern of connections within the network. We would like to speculate that our mechanism of orientation and direction selectivity arises early and only subsequently the afferent and horizontal connections develop in an activity-dependent way. This development could be driven by either visual experience or by spontaneous activity waves in the retina which were observed in kittens even before opening of the eyes (25). In the maturing cortex the connections then become orientation

specific in register with the orientation preference of the neuron's responses (26-30). If the general layout of local intra-cortical connections remains the same at the initial stages of development, our model could explain the remarkable stability of visual maps observed in the experiments (9-11). Our results are also compatible with the finding that kittens raised with strabismus have only a single PO map that is continuous across the segregated monocular domains of the two eyes (31). We emphasize that the network mechanism described above is responsible for the appearance of both the selectivities of single units and the structure of the PO map. This aspect of the model distinguishes it from the previous suggestion of Rojer and Schwartz (20) who pointed out that experimentally observed OP maps could result from random distribution of preferred orientations of single units due to bandpass filtering, caused e.g. by the technique of optical imaging.

The crucial assumption of the model pertained to the mexican-hat form of the connections. The strength of the connections has to be sufficiently strong, which results in the patchy activity states of the network in response to spatially extended stimuli. There is currently no detailed enough data on the connectivity in the primary visual cortex at early stages of the development which could either confirm or reject these assumptions. Our results should therefore be taken more as a proof of the possibility than as a realistic type of modeling which is generally not yet feasible for the network phenomena. We emphasize however the robustness of the resulting appearance of the maps to variations of the network parameters.

Finally, in our network the lateral connections determine the overall, patchy, shape of the activity state of the network for any spatially extended stimulus. The precise geometry

of the visual input is only effective in selecting the exact locations of the patches. This is a very different scenario from the intuitive one according to which the activity in the primary visual cortex should resemble the visual input. It would be extremely interesting to check with modern imaging techniques if indeed our prediction is true and furthermore whether the maturation of cortex induces a transition to the more intuitive regime of activity in which the visual input more effectively determines the population response of the cortex.

METHODS

We simulated a network of 128 by 128 units arranged on a two-dimensional rectangular surface. Each unit j is described by its activity f_j (firing rate), which evolves according to the inputs received from both geniculate afferents and other units in the network (32,33):

$$\tau \frac{df_j}{dt} = -f_j + g(I_j) \quad (1)$$

$$g(I_j) := s \cdot (I_j - t_f) \quad \text{for } I_j > t_f, \text{ and } 0 \text{ otherwise,} \quad (2)$$

where the piecewise linear gain function g with threshold t_f and slope s models the firing activity in dependence on the total synaptic input current $I_j = I_{a,j} + I_{l,j}$, which has contributions from external afferents, $I_{a,j}$, and lateral connections, $I_{l,j}$, within the network. τ is a time constant which has been set to 5 time units throughout our simulations.

Intracortical input is provided by the other units in the network:

$$I_{l,j} = \sum_k \omega_{j,k} f_k \quad (3)$$

The interaction strength $\omega_{j,k}$ between two units at cortical sites \mathbf{r}_j and \mathbf{r}_k is determined by

the following expression

$$\begin{aligned}\omega_{j,k} &= W_e(\mathbf{r}_j - \mathbf{r}_k) + \eta_e(j, k)\sqrt{W_e(\mathbf{r}_j - \mathbf{r}_k)} \\ &- W_i(\mathbf{r}_j - \mathbf{r}_k) + \eta_i(j, k)\sqrt{W_i(\mathbf{r}_j - \mathbf{r}_k)}\end{aligned}\quad (4)$$

$$W_e(\mathbf{r}_j - \mathbf{r}_k) = \frac{J_e}{2\pi\sigma_e^2} \exp\left(-\|\mathbf{r}_j - \mathbf{r}_k\|^2/(2\sigma_e^2)\right) \quad (5)$$

$$W_i(\mathbf{r}_j - \mathbf{r}_k) = \frac{J_i}{2\pi\sigma_i^2} \exp\left(-\|\mathbf{r}_j - \mathbf{r}_k\|^2/(2\sigma_i^2)\right) \quad , \quad (6)$$

where $\eta_e(j, k)$ and $\eta_i(j, k)$ are drawn from a Gaussian distribution with zero mean and a standard deviation $\eta\sqrt{W_e(0)}$ and $\eta\sqrt{W_i(0)}$, respectively. This choice results in a noisy profile of the interaction strength having the shape of a difference of two-dimensional Gaussian functions (mexican hat). The square root factors in the RHS of Eq. (4) indicate that the relative variability in the connection strengths grows with increasing distance between the corresponding columns, due to decrease in connection probability between pairs of single neurons.

Afferent input to unit j is provided retinotopically by a specific region with center \mathbf{R}_j within the visual field (VF),

$$I_{a,j} = \frac{J_a}{2\pi\sigma_a^2} \int_{VF} S(\mathbf{R}) \cdot \exp\left(-\frac{\|\mathbf{R} - \mathbf{R}_j\|^2}{2\sigma_a^2}\right) d\mathbf{R} \quad (7)$$

where $S(\mathbf{R})$ is the visual stimulus at position \mathbf{R} in the visual field VF. In all of our simulations, the centers of input fields \mathbf{R}_j , as well as the cortical units \mathbf{r}_j , were distributed on a regular rectangular lattice having the same dimensions as the cortical lattice. The parameters σ_i , σ_e , and σ_a denote the length scales of the inhibitory and excitatory interactions, and the width of the afferent connection's arbor, respectively. Periodic boundary conditions were used for the cortex and the stimuli to avoid perturbation of the results by geometrical

constraints (34).

We considered two types of stimuli S - full-sized gratings S_g and localized spots S_b and bars (not shown). In the first case, the stimulus is a sinusoidal grating with period Λ , orientation Φ , and velocity v

$$S_g(\mathbf{R}) := S_0 + S_1 \cdot \cos\left(\frac{2\pi(l_x + vt)}{\Lambda}\right) \quad (8)$$

$$l_x := R_x \cos(\Phi) + R_y \sin(\Phi) \quad , \quad (9)$$

where S_0 denotes the average luminance, S_1 the contrast of the stimulus, $\mathbf{R} = (R_x, R_y)$ a position in the VF, and t the time. In the second case, the stimulus is a circular spot of size σ , centered at \mathbf{R}_k

$$S_b(\mathbf{R}) := S_0 + S_1 \exp\left(-\frac{\|\mathbf{R} - \mathbf{R}_k\|^2}{2\sigma^2}\right), \quad (10)$$

where \mathbf{R}_k runs over all positions where localized stimuli were presented.

To obtain the angle maps, full-sized gratings moving in $N = 16$ different directions covering the full circle, $\Phi(n) = 2\pi n/N$, were presented to the network. For each of these stimuli, after an initial time interval of $T_0 = 500$ time units which was long enough for the activity patterns to build up, one single condition activity map $A_{j,n}$, $n = 1, \dots, N$ has been obtained by averaging the resulting activities $f_{j,n}(t)$ over a time interval of $T = 1000$ time units

$$A_{j,n} = \frac{1}{T} \sum_{t=T_0}^{T_0+T} f_{j,n}(t). \quad (11)$$

Single condition orientation maps $A_{j,m'}$, $m = 1, \dots, N/2$ were obtained by summing up the corresponding single condition direction maps, $A_{j,m'} = 0.5(A_{j,m} + A_{j,2m})$. Preferred

direction Θ_j of each unit j was obtained by vectorially summing up the averaged activities for each direction of motion. Similarly, the preferred orientations Φ_j were obtained by the same procedure after first averaging the activity over two opposite directions of motion for each orientation of the grating (see e.g. (22))

$$\Theta_j = \arg \left\{ \frac{1}{N} \sum_{n=1}^N A_{j,n} \exp(i\Phi(n)) \right\} \quad (12)$$

$$\Phi_j = \arg \left\{ \frac{1}{N} \sum_{n=1}^N A_{j,n} \exp(2i\Phi(n)) \right\} \quad (13)$$

To obtain the single unit receptive fields, we applied a small non-oriented stimulus S_b at positions \mathbf{R} on a regular lattice, sampling the whole visual field VF, thus leading to the activity distributions $A_j^{RF}(\mathbf{R})$. The receptive field of a unit j was then analyzed as follows: with $\text{sgn}(x) = 1$ for $x > 0$ and 0 otherwise, the sizes (average diameters) d_j of the receptive fields in units of the lattice unit length were computed as $d_j = \sqrt{4/\pi \left(\int_{VF} \text{sgn}(A_j^{RF}(\mathbf{R})) d\mathbf{R} \right)}$.

Our standard parameter set for the simulations was $s = 0.1$, $t_f = 0$, $J_e = 40$, $J_i = 60$, $J_a = 200$, $\sigma_e = 5.6$, $\sigma_i = 10$, $\sigma_a = 5$, $S_0 = 1$, $S_1 = 1$, $\Lambda = 18$, $v = 0.8$, $\eta = 0.2$. For the presentation of localized non-oriented stimuli, we used $S_0 = 0$, $S_1 = 5$, and $\sigma_a = \sigma_b = 3$ for the data shown in Fig. 4. We presented the localized stimuli at 64 by 64 positions in the VF, in order to approximate the integrals in the expressions used to calculate the receptive sizes d_j . The differential equations for network activity were integrated using a fourth-order Runge-Kutta integration scheme with $dt = 1$.

References

- [1] Hubel, D. H. & Wiesel, T. N. Receptive fields, binocular interaction and functional architecture in the cat's visual cortex. *J. Physiol. (London)* **160**, 106-154 (1962).
- [2] Blasdel, G.G. & Salama, G. Voltage-sensitive dyes reveal a modular organization in monkey striate cortex. *Nature* **321**, 579-585 (1986).
- [3] Grinvald, A. et. al. Functional architecture of cortex revealed by optical imaging of intrinsic signals. *Nature* **324**, 351-354 (1986).
- [4] von der Malsburg, C. (1973) *Kybernetik* **14**, 85-100.
- [5] Swindale, N.V. A model for the formation of orientation columns. *Proc. Roy. Soc. London B* **215**, 211-230 (1982).
- [6] Obermayer, K., Ritter, H. & Schulten, K. A principle for the formation of the spatial structure of cortical feature maps. *Proc. Natl. Acad. Sci. USA* **87**, 8345-8349 (1990).
- [7] Miller, K.D. A model for the development of simple cell receptive fields and the ordered arrangement of orientation columns through activity-dependent competition between on- and off-center inputs. *J. Neurosci.* **14**, 409-441 (1994).
- [8] Wolf, F. & Geisel, T. Spontaneous pinwheel annihilation during visual development. *Nature* **395**, 73-78 (1998).
- [9] Gödecke, I., Kim, D.-S., Bonhoeffer, T. & Singer, W. Development of identical maps for two eyes without common visual experience. *Eur. J. Neurosci.* **9**, 1754-1762 (1997).

- [10] Gödecke, I. & Bonhoeffer, T. (1996) *Nature* **379**, 251–254.
- [11] Crair, M.C., Gillespie, D.C. & Stryker, M.P. The role of visual experience in the development of columns in cat visual cortex. *Science* **279**, 566-570 (1998).
- [12] Sompolinsky, H. & Shapley, R. New perspectives on the mechanisms for orientation selectivity. *Curr. Opin. Neurobiol.* **7**, 514-522 (1997).
- [13] Ben-Yishai, R., Bar-Or, R. & Sompolinsky, H. Theory of orientational tuning in visual cortex. *Proc. Natl. Acad. Sci. USA* **92**, 3844-3848 (1995).
- [14] Somers, D.C., Nelson, S.B. & Sur, M. An emergent model of orientation selectivity in cat visual cortical simple cells. *J. Neurosci.* **15**, 5448–5465 (1995).
- [15] Ahmed, B., Anderson, J., Douglas, R., Martin, K. & Nelson, J. Polyneuronal innervation of spiny stellate neurons in cat visual cortex. *J. Comp. Neurol.* **341**, 39-49 (1994).
- [16] Amari, S. Dynamics of pattern formation in lateral-inhibition type neural fields. *Biol. Cybern.* **27**, 77-87 (1977).
- [17] Tsodyks, M. V. & Sejnowski, T. J. Associative memory and hippocampal place cells. *Int. J. Neural Sys.* **6**, 81-86 (1995).
- [18] Bonhoeffer, T. & Grinvald, A. Orientation columns in cat are organized in pin-wheel like patterns. *Nature* **353**, 429-431 (1991).
- [19] Obermayer, K. & Blasdel, G. Geometry of orientation and ocular dominance columns in monkey striate cortex. *J. Neurosci.* **13**, 4114-4129 (1993).

- [20] Rojer, A.S. & Schwartz, E.L. Cat and monkey cortical columnar patterns modeled by bandpass-filtered 2D white noise. *Biol Cybern.* 1990;62(5):381-91. *Biol. Cyb.* **62**, 381-391 (1990).
- [21] Swindale, N.V., Matsubara, J.A & Cynader, M.S. Surface organization of orientation and direction selectivity in cat area 18. *J. Neurosci.* **7**, 1414-1427 (1987).
- [22] Shmuel, A. & Grinvald, A. Functional organization for direction of motion and its relationship to orientation maps in cat area 18. *J. Neurosci.* **16**, 6945–6964 (1996).
- [23] Das, A. & Gilbert, C. Distortions of visuotopic map match orientation singularities in primary visual cortex. *Nature* **387**, 594-598 (1997).
- [24] Ernst, U., Pawelzik, K., Tsodyks, M., & Sejnowski, T. Relation between retinotopical and orientation maps in visual cortex. *Neur. Comp.* **11**, 375-379 (1999).
- [25] Maffei, L. & Galli-Resta, L. Correlation in the discharges of neighboring rat retinal ganglion cells during prenatal life. *Proc. Natl. Acad. Sci. USA*, **87**, 2861-2864 (1990).
- [26] Gilbert, C & Wiesel, T. Columnar specificity of intrinsic horizontal and corticocortical connections in cat visual cortex. *J. Neurosci.* **9**, 2432-2442 (1989).
- [27] Löwel, S. & Singer W. (1992) *Science* **255**, 209–212.
- [28] Malach, R., Amir, Y., Harel, M. & Grinvald, A. Relationship between intrinsic connections and functional architecture revealed by optical imaging and in vivo targeted biocytin injections in primate striate cortex. *Proc. Natl. Acad. Sci. USA* **90**, 10469-10473 (1993).

- [29] Reid, R.C. & Alonso, J.M. Specificity of monosynaptic connections from thalamus to visual cortex. *Nature* **378**, 281-284 (1995).
- [30] Ferster, D., Chung, S. & Wheat, H. Orientation selectivity of thalamic input to simple cells of cat visual cortex. *Nature* **380**, 249-252 (1996).
- [31] Löwel, S., Schmidt, K. E., Kim, D.-S., Wolf, F., Hoffsummer, F., Singer, W. & Bonhoeffer, T. (1998) *Europ. J. Neurosci.* **10**, 2629–2643.
- [32] Wilson, H. & Cowan, J. (1973) *Biol. Cyb. (Kybernetik)* **13**, 55–80.
- [33] Grossberg, S.(1988) *Neural Networks* **1**, 17-61.
- [34] Wolf, F., Bauer, H.-U., Pawelzik, K. & Geisel, T. (1996) *Nature* **382**, 306–307.
- Shouval, H.Z, Goldberg, D.H, Jones, J.P, Beckerman, M. & Cooper, L.N. Structured long-range connections can provide a scaffold for orientation maps. *J. Neurosci.* **20**, 1119-1128 (2000).

Acknowledgments

We thank S. Hoshtein, A. Shmuel, S. Löwel, W. Singer and F. Wolf for comments on an earlier draft of the manuscript. This work was supported by grants from Max-Planck-Gesellschaft, Deutsche Forschungsgemeinschaft, Office of Naval Research, Minerva foundation and the Hanse Wissenschaftskolleg.

FIGURE LEGENDS

Figure 1 (a) The average inter-unit connection strength strength (normalized) as a function of the distance between the units (same scale as in (b)). The colors green, red, and black distinguish excitatory, inhibitory, and the sum of excitatory and inhibitory connection strengths, respectively. (b) Activity state $A_j, j = 1, \dots, 128 \times 128$ of the network in response to a uniform stimulation of all of the units with the intensity $I_{a,j} \equiv 2$. Activation levels are coded in grey shades.

Figure 2

Formation of PO maps.

(a) Activity patches for $M = 8$ different orientations of the full-sized grating, $A_{j,m'}, m = 1, \dots, 8$. Each panel represents the full network, activation levels are coded in grey shades as in Fig. 1. (b) The color-coded angle map of preferred orientations Φ_j . (c) TUNING CURVES OF SINGLE UNITS - TO BE COMPLETED.

Figure 3

Direction preference of the cortical columns shown in Fig. 2, obtained in the same computer simulation. (a) Closeup of the differential direction map between the activities $A_{j,m}$ produced by an oblique grating moving up and to the left (purple), and by the activities $A_{j,2m}$ obtained by moving the stimulus in the opposite direction (green). The total activity $A_{j,m'}$, obtained by summing up over the two opposite direction of motion, is coded in grey shades (white=weak activation, black=strong activation). Columns responding preferentially to the

up-left (down-right) movement are marked with purple (green) arrows. **(b)** The color-coded angle map of the preferred directions, $\Theta_j, j = 1, \dots, N_x \cdot N_y$. The black frame marks the region from which **(a)** has been chosen.

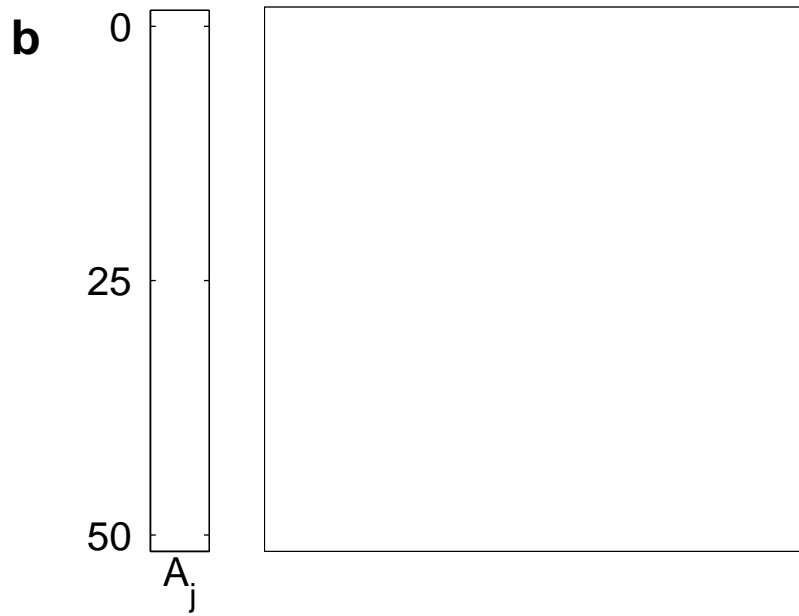
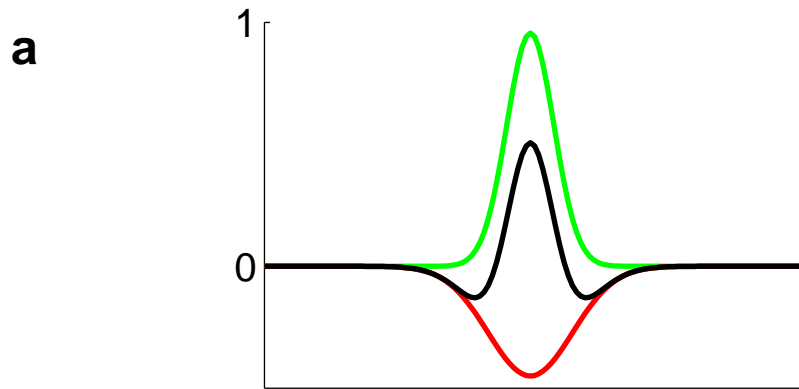
Figure 4

Relationship between the distance of the receptive fields and the difference in preferred orientation for pairs of cortical units. For a random choice of pairs (j, k) of units, the distance C_{jk} between their receptive fields, normalized by their sizes (diameters), $C_{jk} := 2\|C_j - C_k\|/(d_j + d_k)$, is plotted against the angle Φ_{jk} between the preferred orientations of the units, $\Phi_{jk} := \|\Phi_j - \Phi_k\|$; for units more than half a hypercolumn apart, the differences in the orientations of neighbouring units between the units j and k were accumulated yielding angles greater than 90 degrees. The solid line indicates the average ratio between the RF movement and the change in orientation of approximately one RF diameter per 87.5 degrees.

Figure 5

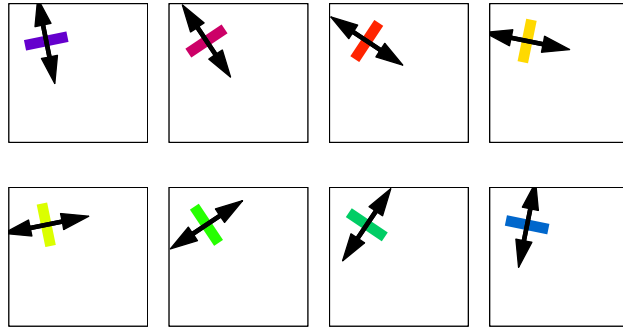
Different regimes of activity for the cortical model in the phase space spanned by the strengths J_e and J_i of the excitatory and inhibitory couplings, respectively. Linear stability analysis yields the upper curve $J_i^u(J_e) = (\alpha J_e)^{1/\alpha} (s\beta)^\beta$ ($\alpha := (\sigma_e/\sigma_i)^2$, $\beta := 1/\alpha - 1$), separating the regime where the network response mainly reflects the input ("linear regime"), from the regime where patchy patterns of excitation like the one shown in Fig. 1 appear as the stable states of the network ("marginally stable regime" [13]). The insets show the eigenvalues of the activity dynamics $\lambda(k)$ as a function of the wave length k , obtained from a stability analysis. The average periodicity of the patchy patterns can be estimated by

evaluating the wave length at which the eigenvalue is at the maximum: $k^2 \approx \frac{2}{\sigma_1^2 - \sigma_e^2}$. Below the lower curve, $J_i^l(J_e) = J_e - 1/s$ the activity diverges (unphysiological regime).

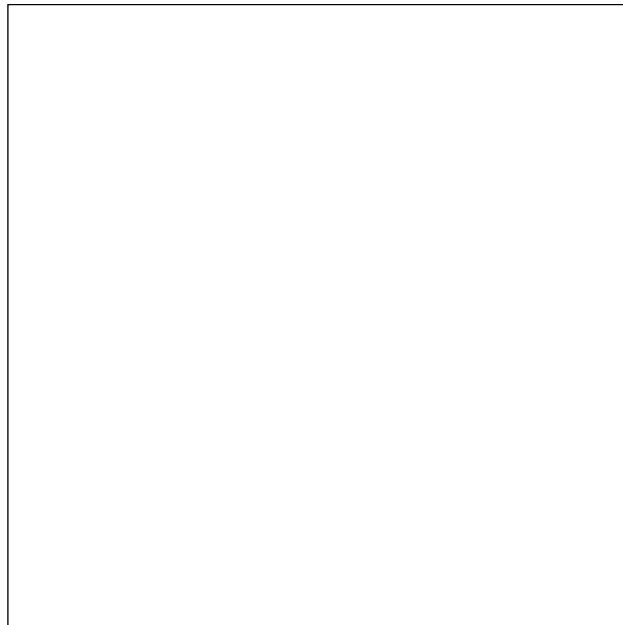


15cm

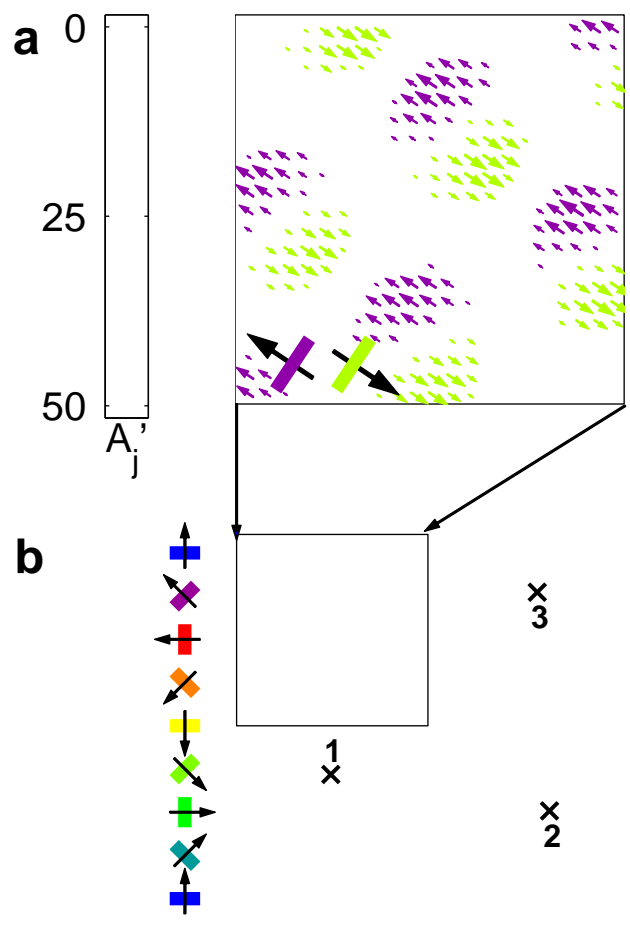
a



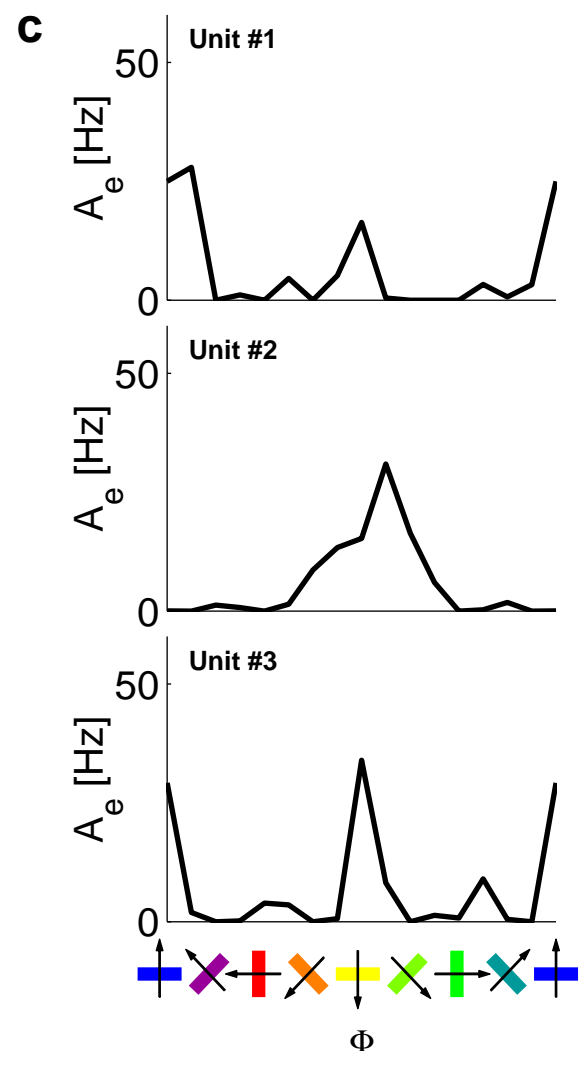
b

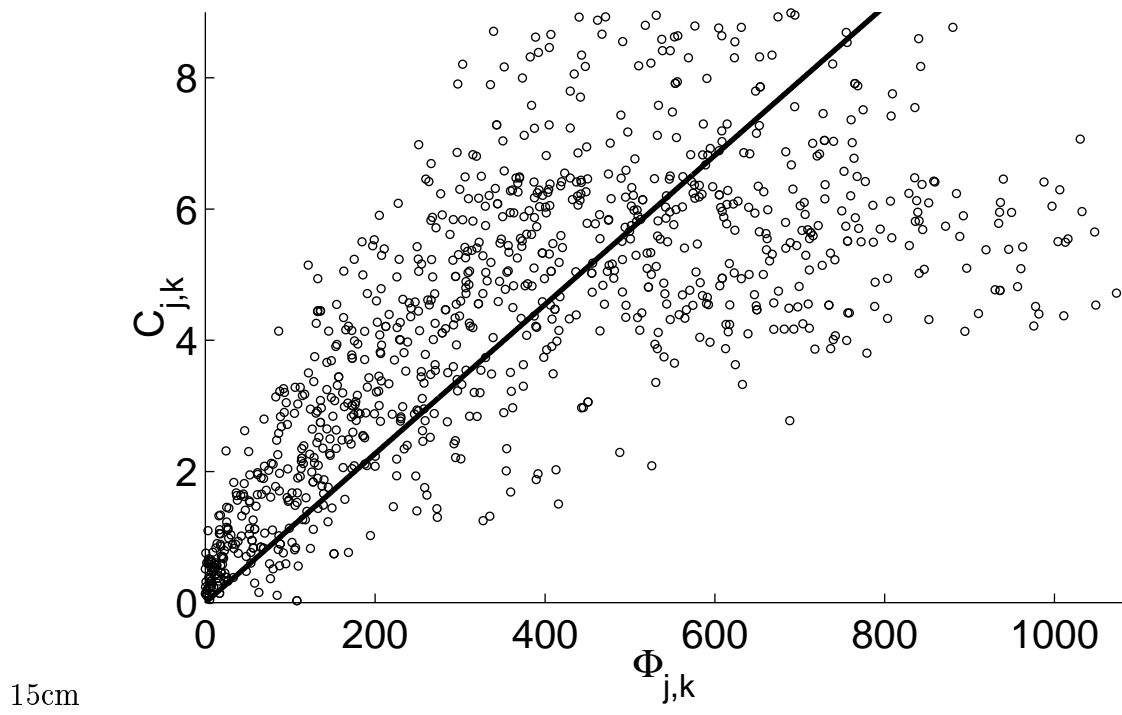


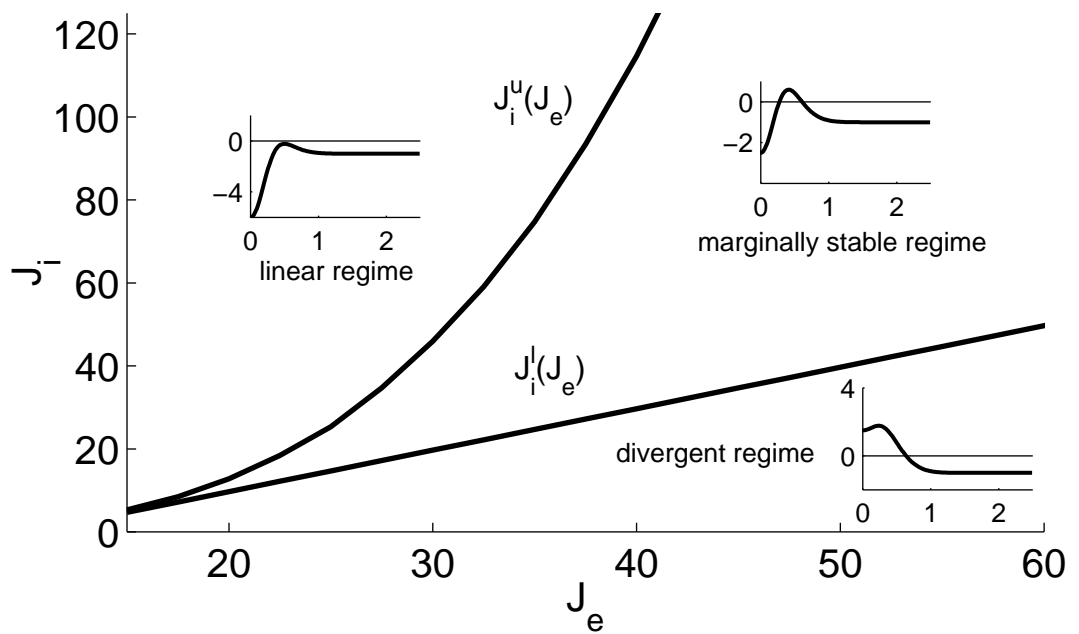
14cm



15cm







15cm